SLAC-PUB-1498
October 1974
(T/E)

REVISION OF BEVATRON BRANCHING RATIO RESULTS ON $K_L^o \to \mu^+\mu^-$ AND $K_L^o \to \pi^+\pi^-$ *

R. C. Field

Stanford Linear Accelerator Center
Stanford University, Stanford, California 94305

ABSTRACT

Results are given of a reanalysis of some data from a Bevatron experiment on the decay modes $K_L^o \to \pi^+\pi^-$, $\pi^\pm\mu^\mp\nu$, $\pi^\pm e^\mp\nu$, and $\mu^+\mu^-$. The ratio $\Gamma(K_L^o \to \pi^+\pi^-)/\Gamma(K_L^o\mu 3 + K_L^o e3)$ is found to be $(2.77 \pm .065) \times 10^{-3}$, so that $\Gamma(K_L^o \to \pi^+\pi^-)/\Gamma(K_L^o \to \text{all})$ is $(1.82 \pm 0.08) \times 10^{-3}$. A limit is obtained for $\Gamma(K_L^o \to \mu^+\mu^-)/\Gamma(K_L^o \to \pi^+\pi^-)$ of $< 1.53 \times 10^{-6}$ (90% C.L.), 24% higher than in the original analysis of this data.

(Submitted to Nuclear Physics.)

*Work supported by the U. S. Atomic Energy Commission.

In the summer of 1972 the CP violating decay mode $K_L^o \to \pi^+\pi^-$ was an uncontroversial if enigmatic highlight of experimental physics. Since then, however, the apparently well measured branching ratio $(K_L^o \to \pi^+\pi^-)/(K_L^o \to \text{all})$[1] has been subjected to serious questioning from several sources.[2] These recent experiments seem to advocate a branching ratio about 35% higher than previously accepted — a discrepancy of perhaps 8 standard deviations. At the same time a large discrepancy appeared between measurements of the branching ratio $(K_L^o \to \mu^+\mu^-)/(K_L^o \to \text{all})$.[3,4] The latter branching ratio is closely related experimentally to the former, and, with the introduction of CP violating amplitudes[5] to explain the unexpected initial dimuon result, the two ratios also became closely coupled theoretically. In the absence of these CP violating amplitudes, a unitarity-based lower bound on the branching ratio of 6×10^{-9} appeared to be violated by the first experiment[3] ($< 1.8 \times 10^{-9}$, 90% C.L.), but not by the second[4] ($9^{+6}_{-3} \times 10^{-9}$).

The 1970 Bevatron experiment[3] on the dimuon ratio yielded a large number of events of the classes $K_L^o \to \pi^+\pi^-$, $\pi^\pm\mu^\mp\nu$ and $\pi^\pm e^\mp\nu$. A reexamination of these data has been carried out in the hope of casting some light on both discrepancies. This is a report of the work.

More specifically, two aspects are discussed, $R_1 = \Gamma(K_L^o \to \pi^+\pi^-)/\Gamma(K_L^o \to \text{all})$, for which only a fraction of the data were used, and $R_2 = \Gamma(K_L^o \to \mu^+\mu^-)/\Gamma(K_L^o \to \pi^+\pi^-)$, which required all the data. There is much in common between the two analyses, and it was felt that the first part could act as an important cross-check of the second. This is particularly true of the simulation program, which could thus be tested against large samples of three decay modes rather than of just one.

Apparatus Performance and Data Reduction

In a series of previous reports[6,7,8] on several aspects of this experiment, descriptions were given of the apparatus, Fig. 1, and its performance. Consequently a brief commentary is adequate here.

A K_L^o beam of momentum 1 GeV/c - 3 GeV/c (Fig. 2) was derived at 3.7° from a copper target at the end of a Bevatron extracted proton beam line. After a magnetically swept, shadow collimated, 7.6 m long beam pipe of solid angle 0.85 msr (the final 2 m in vacuo), the K_L^o beam traversed a 5.8 m long evacuated decay volume. Beyond this it passed through a shielded channel between the two arms of the apparatus to a beam dump. The beam typically contained about 10^6 K_L^o from each Bevatron pulse and perhaps 500 times this number of neutrons and gammas.

The K_L^o decays which the twin-spectrometer apparatus detected and recorded had the following properties:

1. One charged particle of each sign entered the appropriate spectrometer magnet and was deflected back and roughly parallel to the beam line.
2. On both sides, after deflection the trajectory passed through a pair of hodoscope counter banks which restricted angles of interest in the horizontal plane to a range of approximately ±45 mr from the direction parallel to the beam line. This was modified for trajectories identified by the Cerenkov counters as electrons to approximately -15 mr to + 45 mr from the beam line, effectively reducing the excessive Ke3 trigger rate. Negative angles signify convergence with the beam line.
3. The trajectories gave signals in aperture-defining counters at the first and second hodoscope banks on each side.
4. The signals from the two sides were closely isochronous (within ±5 ns approximately).

This trigger scheme restricted the range of acceptable secondary particles to those with transverse momenta in the plane of the apparatus greater than about 195 MeV/c. Consequently the eligible decay modes were Ke3, Kμ3, and charged two body channels.

To identify the secondary particles, Cerenkov counters (Freon 12 at 1 atmosphere) signalled the passage of electrons. Three photomultiplier tubes were used in each counter. To veto electrons in the angular range -15 mr to -45 mr convergent to the beam line (as mentioned above), only the central tube was used, giving an effective veto efficiency of about 95%. The Cerenkov counters were calibrated in an electron beam to have efficiency > 99.6% for detecting electrons. No method was found, however, to monitor the efficiency to better than 5 or 10% during operation. From test beam results and from data from $K\mu 3$ and $K\pi\pi$ events the accidental mislabeling of μ and π as electrons was (2.14 ± 0.20)%.

The excellent performance of the range telescopes for the range-momentum identification of muons has been detailed elsewhere.[7] Although the detection efficiency for muons is essentially 100% there remains a momentum-dependent probability of several percent that a pion (for example by decaying in flight) will exhibit the range of a muon of the same momentum.

The wire spark chamber spectrometers measured the momenta of the trajectories to ± 0.6% on average, and from this measurement and reconstruction of the decay vertex position several kinematic quantities were calculated. On the assumption that the decay process involved only two secondaries, the K_L^o trajectory was calculated and could be tested to see whether it appeared to originate at the target. On the further assumption of identity of the secondaries an invariant mass for the reaction was calculated. The typical mass resolution for the K_L^o mass was ±1.4 MeV/c^2 R. M. S.

The invariant mass and target properties were used to identify the two body processes, in particular $K_L^o \rightarrow \pi^+\pi^-$, and unacceptable candidates were then treated as three-body decays.

Making tentative identification by the presence or absence of a Cerenkov signal, Ke3 and Kμ3 decays were reconstructed, albeit with the familiar quadratic ambiguity of two possible solutions for the K_L^o momentum (p_K) and the Dalitz plot position.

After bulk processing to this condition the reconstructed data were available for comparatively inexpensive further analysis.

$\Gamma(K_L^o \rightarrow \pi^+\pi^-)/\Gamma(K_L^o \rightarrow \text{all})$: Analysis of Data Sample

To examine the relative abundances of the three decay schemes in question only a fraction of the available data was needed. In examination of the reconstructed data an inefficiency was found in the rear left side of the apparatus, exhibiting itself as marked broad flattening of the track distributions in the planes of the various detectors. The effect became progressively more noticeable in the last 60% of the data. Although Monte Carlo studies indicate that the relative acceptances of $K_L^o \rightarrow \mu^+\mu^-$ and $K_L^o \rightarrow \pi^+\pi^-$ were affected by less than 1% by this effect, the data sample selected here was chosen from an early sequence of runs which showed good symmetry between the two sides.

The general philosophy was adopted that the 2π mode should be identified as in the $K\mu\mu : K\pi\pi$ analysis by the kinematic quantities invariant mass and K_L trajectory consistency with the position of the production target. The three-body modes would be identified as far as possible by range and Cerenkov information, with recourse to kinematic tests minimized, contrary to recent practice in the field.

Certain tests and cuts (Table I) were applied to all data. An examination was made of the precision with which the segments of trajectories in front of and behind the magnets coincided with each other at the magnet mid-plane. Liberal limits on the discrepancy were set, reducing the incidence of decay in flight in the sample. A cut was also imposed on the separation of the two trajectories at their "vertex", again liberal and effective only against decays in flight.

A fiducial volume was defined for the vertex positions to help eliminate low level backgrounds to the $K_L \to \mu\mu$ search. Its importance to this discussion is that any contamination by K_S^o production at the front walls of the decay volume was eliminated, as was a background of events caused by neutron interactions there. This second class could not be identified as K_L^o decays in any case.

Further cuts applied to all data discussed here were secondary momentum limits of 550-1800 MeV/c, rejecting only a few percent of events, and cuts applied to the intersection of the projected trajectory with the front face of the range telescope.

A profile of one of the range telescopes is shown in Fig. 3. A detailed analysis of the multiple scattering of muons in these instruments was carried out and subsequently checked by using a spark chamber behind the initial lead-graphite degrader thickness.[9] On the basis of these results it was decided that the probability of a muon multiple scattering out of the telescope at an apparent range too short for the muon classification was adequately small if trajectories passing within a 10 cm margin around the edge of the face of the telescope were rejected. To be certain about this the analysis was performed with both 12.5 cm and 7.5 cm margins.

The criterion employed in muon identification made use of an empirically corrected range-momentum relation[7] and straggling width. Allowing for the asymmetry in the range straggling and slight counter inefficiencies a cutoff was made at more than approximately 3 counters short of the expected μ range — see Fig. 4.

The use of the Cerenkov counter partially to eliminate the large number of converging electron trajectories was noted above. The resultant complications in analysis were much reduced by eliminating from consideration all trajectories with a Cerenkov signal converging more steeply than 15 mr with the beam axis.

Based on combinations of the various signatures chosen for event identification the data were divided into several categories (Table II). The various distributions of the small ambiguous categories were examined in detail to attempt to estimate the make-up of their populations. For the two cases of range telescope fiducial margin cuts mentioned above the population distribution is given in Table III.

Some histograms are shown to illustrate the appearance of the data. The clean separation of $K\pi\pi$ events with a range cut exclusive of muons can be seen in Fig. 5a, while Fig. 5b indicates the occurrence of some $K\pi\pi$ events with one range within the muon criterion — over a background of $K\mu3$ events. An indication of the sharpness of the muon range curve is given in Fig. 4. The observed range minus the expected range is plotted for part of the data, and the muon identification cutoff is indicated.

The errors quoted represent statistical and conservatively estimated systematic uncertainties for the separation. Corrections are necessary for the effect of π decay in flight, which can for example contaminate $K\mu3$ with some $K\pi\pi$ category failures, for the small losses of muons by multiple scattering, for the effects of the Cerenkov veto — even by accidentals — on ambiguous categories involving the Cerenkov counters, and for bremsstrahlung effects.

The category of uncertain identification, XXX, shows evidence that at least a major fraction of it consists of $K\pi\pi$ events where a π has decayed in flight roughly in the plane of the apparatus. The vertical "target" distribution is somewhat peaked, whereas its horizontal counterpart is flat by comparison with acceptable $K\pi\pi$ events. The invariant mass distribution shows evidence of a very broad peak rather lower than the K mass, not resembling the distribution for any other identification category but consistent with computer simulation studies of decay in flight. The range distributions are broader than those of pions in clearly identified K events — which presumably have decayed in flight less frequently than the XXX candidates. Finally, the distribution in convergence of the tracks in the rear of the apparatus shows a fraction of the category converging strongly on the beam line, consistent with decay in flight before passing the magnets. No evidence is found from the shapes of Dalitz plots of such events that they exhibit any characteristics of the semi-leptonic decays. It is believed that they do not represent any significant loss from the clearly constrained categories used for the data and its simulation. This category corresponds to about 3.4% of the final corrected number of $K\pi\pi$ events.

Data Simulation

To make use of these numbers for branching ratio evaluations it was, of course, necessary to simulate the response of the apparatus to the various decay modes. The program used for this was also used in the $\mu\mu:\pi\pi$ analysis discussed below.

The apparatus was represented by realistic geometrical constructions. The magnetic fields were represented for horizontal trajectory components by a simple thin prism approximation, but a detailed study was made to allow satisfactory representation of the vertical focusing. Because of the uniformity of the field integrals to better than $\pm 1\%$ over 95% of the useful aperture, this approach gave excellent results.

Resolution functions for the spectrometers and multiple scattering in the hodoscope-Cerenkov counter region were included at least in approximation. Use was made of the observed angular distributions in the hodoscopes as projected by the spark chambers to adjust the two field strengths in the simulation to the correct values, and the locations of the hodoscope banks were also determined most accurately from the data.

The K_L^o momentum spectrum was determined by comparison of the data and simulation for $K\pi\pi$ events with corrections applied for π decay in flight.

For reasons of economy, the effects of decay in flight were evaluated in a separate program. This had the disadvantage that direct graphical comparison between data and simulation was only approximate. In the case of the two body decay, however, the approximation is very good if the simulated K spectrum has not been corrected for decay in flight losses — essentially because the loss of events is largely uncoupled from the pion momentum by the correlation between the momentum dependent decay probabilities on the two sides. This establishes confidence that no systematic mischief was introduced by the separation.

Radiative corrections[10] were applied to the Ke3 rate calculation. The possibility of loss of data because of the soft photon emission (not accounted for in Ginsberg's formulae) was investigated and found to be negligible within the uncertainties of the work. The size of the radiative correction is (-4.4)% and its error is assumed to be $\pm 0.5\%$ or less.

Despite the approximation involved, comparisons of data and simulation before correction for decay in flight are shown in graphs starting at Fig. 6. This displays the decay point distribution along the length of the decay volume for $K\pi\pi$ events. A secondary momentum spectrum is shown in Fig. 7, while a hodoscope trigger angle distribution appears in Fig. 8.

Similar distributions have been examined for the $K\mu 3$ and Ke3 data (e.g., Fig. 9), along with Dalitz plot projections, and also other spacial distributions and numerous correlations. The agreement between data and simulation is satisfactory except for the trigger angle distribution of pions from Ke3 on the right side of the apparatus, Fig. 9(b). Although this nonstatistical discrepancy is unexplained, there is no further indication of a systematic effect influencing the branching ratio measurements. It is concluded that the simulation program represents the data well and that for the few parameters on which accuracy depends (for example field strength) uncertainties can reliably be evaluated.

Losses caused by decay in flight of pions were calculated with the help of modified versions of the simulation routines. The loose cuts applied to the events tend to fall in the middle of the distributions of events with a decay in flight. This, plus the approximate treatment of the resolution functions means that the systematic errors associated with the decay in flight corrections are comparatively large.

Results

In quoting the geometrical acceptance efficiencies of $K\mu 3$ and Ke3 it is convenient to give values relative to the $K\pi\pi$ efficiency under the same conditions. In the cases where 7.5 cm and 12.5 cm range telescope margin cuts were applied, the $K\pi\pi$ absolute efficiencies were 2.4×10^{-3} and 1.9×10^{-3} respectively for the approximately 10% of decays occurring in the decay volume.

The observed samples of the three decay modes and the corrections applied to them are shown in Table IV.

Note that the correction for the Cerenkov counter induced losses of $K\pi\pi$ events was estimated directly from the category $K\pi\pi C$ and the knowledge of the hodoscope angle distribution. A similar loss of $K\mu3$'s was checked in the categories $K\mu3C$ and indicated that the probability of a Cerenkov signal was the same — $(2.1 \pm 0.2)\%$ — for muons and pions.

For $K\mu3$ events, calculation[9] indicates that 1.52% of muons should be lost from the sample by multiple scattering from the fiducial volume inside the projected 7.5 cm range telescope margin. From the data with the 12.5 cm cut the loss should be 0.30%. A comparison of the data and simulation programs for the two cases agrees with this estimate within statistics.

One unique correction for the Ke3 events was estimated by simulation. This was the loss brought about by bremsstrahlung before the second hodoscope. The resulting spectrum of "softened" electrons could, of course, experience enough multiple scattering to escape the apparatus trigger.

Only about 10% of the available Dalitz Plot phase space for the $K\mu3$ and Ke3 decay modes was accessible in this experiment. This, together with the strong dependence of the rates[*11] on the form factor parameters $\xi(0)$ and λ_+, precluded a direct measurement of the relative branching ratio. It was possible, however, to determine what values of the form factors are compatible with the observed ratio. This effectively has meant using the simulation program to determine the dependence of the acceptances on $\xi(0)$ and λ_+. Then, for comparison with experiment, the expected ratio was plotted as a function of these parameters. The 12.5 cm and 7.5 cm cuts gave completely compatible results. The choice was made, however, to apply the 12.5 cm cut to the $K\mu3$ data, thus reducing the correction for multiple scattering in the degrader. An example of the acceptance relative to $K\pi\pi$ for the same cuts is quoted below.

In the Ke3 case there was no reason to so restrict the acceptance and so the 12.5 cm cut was imposed. The Ke3 acceptance is quoted with respect to

---

* $\Gamma(K_L\mu3)/\Gamma(K_Le3) = 0.6452 + 0.1246\,\mathrm{Re}\xi + 0.0186\,|\xi|^2 + 1.3162\lambda_+ + 0.437\lambda_-\,\mathrm{Re}\xi + 0.0064\lambda_+\mathrm{Re}\xi$.

the $K\pi\pi$ acceptance for a 12.5 cm cut.

$$K\mu 3: \quad \eta_\mu = (1.515 \pm 0.018) \times 10^{-2} \qquad (\xi(0) = -0.25,\ \lambda_+ = 0.03)$$

$$Ke3: \quad \eta_e = (6.15 \pm 0.17) \times 10^{-3} . \qquad (\xi(0) = -0.25,\ \lambda_+ = 0.03)$$

The errors represent the statistical and estimated systematic uncertainties in the simulation:

stat: $K\pi\pi \pm 0.6\%$; $K\mu 3 \pm 0.825\%$; $Ke3 \pm 0.72\%$

syst: $\pi\pi/\mu 3 \pm 0.68\%$; $\pi\pi/e3 \pm 2.55\%$; $\mu 3/e3 \pm 2.0\%$

The systematic errors allow for uncertainties in the spectrometer field strengths, hodoscope position, K_L^o spectrum, etc. The $\pm 0.22\%$ field strength uncertainty in each magnet was dominant and by itself contributed

$\pi\pi/\mu 3 \pm 0.4\%$; $\pi\pi/e3 \pm 2.1\%$; $\mu 3/e3 \pm 1.7\%$

Note that an error in the field strength which would cause $\Gamma(K\mu 3)/\Gamma(Ke3)$ to be measured too high would also cause the other ratios to be too high.

From these results a locus of acceptable values in $(\xi(0), \lambda_+)$ space is obtained, represented by

$$\xi(0) = (0.65 \pm 0.38) - 12.75\ \lambda_+ \quad (\lambda_- \text{ assumed} = 0.0)$$

For example $\xi(0) = 0.2675$ if $\lambda_+ = 0.03$, corresponding to the branching ratio

$$\Gamma(K\mu 3)/\Gamma(Ke3) = 0.7194 \pm 0.049$$

The result given by the Particle Data Group[11] is

$$\Gamma(K\mu 3)/\Gamma(Ke3) = 0.6933 \pm 0.019$$

In view of the notoriety of these decay modes, the arbitrary decision was made to take the semileptonic modes together in quoting a branching ratio for the $\pi^+\pi^-$ channel. The sum of the semileptonic rates has been assumed fixed relative to the 3π channels independent of any assumption about the form factors. From the Particle Data Tables

$$\Gamma(K\mu 3 + Ke3)/\Gamma(K \rightarrow \text{all}) = 0.657 \pm 0.01 \, .$$

Then, for

$$\xi(0) = -0.25, \; \lambda_+ = 0.03, \; \lambda_- = 0.0 \;\; ,$$

$$\Gamma(K \rightarrow \pi\pi)/\Gamma(K\mu 3 + Ke3) = (2.767 \pm 0.065) \times 10^{-3},$$

or

$$R_1 = \Gamma(K \rightarrow \pi\pi)/\Gamma(K \rightarrow \text{all}) = (1.818 \pm 0.050) \times 10^{-3} \; .$$

The sensitivity to the form factors is quite strong,

$$\frac{1}{R_1} \frac{\Delta R_1}{\Delta \xi} = -0.042, \qquad \frac{1}{R_1} \frac{\Delta R_1}{\Delta \lambda_+} = -2.53.$$

The values $\xi(0) = -0.25 \pm 0.5$, $\lambda_+ = 0.03 \pm 0.01$ are imposed as representative of a consensus of available results. Taking these errors in quadrature with the other experimental uncertainties,

$$\Gamma(K_L^o \rightarrow \pi^+\pi^-)/\Gamma(K_L^o \rightarrow \text{all}) = (1.818 \pm 0.078) \times 10^{-3}$$

$\underline{\Gamma(K_L^o \rightarrow \mu^+\mu^-)/\Gamma(K_L^o \rightarrow \pi^+\pi^-)\text{: Analysis of the Data Sample}}$

The first published result of the data being used here was the limit $\Gamma(K_L^o \rightarrow \mu\mu)/\Gamma(K_L^o \rightarrow \text{all}) < 1.8 \times 10^{-9}$ (90% C.L.)[3]. A subsequent measurement[4] reported $\Gamma(K_L^o \rightarrow \mu\mu)/\Gamma(K_L^o \rightarrow \text{all}) = (9.1^{+6}_{-3}) \times 10^{-9}$ based on 9 events, in violent disagreement. Both these results assumed $R_1 = \Gamma(K_L^o \to \pi\pi)/\Gamma(K_L^o \to \text{all}) = (1.57 \pm 0.05) \times 10^{-3}$.

In the original analysis of the Bevatron experiment the two-body decay candidates were selected by imposing cuts on the various available distributions of the reconstructed event parameters. The reanalysis presently reported, however, was modeled as far as possible after that of the contradictory experiment in the unfulfilled hope of gaining an insight into possible systematic biases at the root of the discrepancy. A χ^2 was calculated for all $\pi\pi$ and $\mu\mu$ candidates, and background rejection was based on this criterion as far as possible. The variables used were:

1 and 2: Transverse horizontal (x) and vertical (y) coordinates of the reconstructed K_L^o trajectory projected back to the production target plane. The distributions of these variables were dependent on the K_L^o momentum (p_K) and were so treated.

3: The difference between y coordinates of the right and left secondary tracks where they appeared to cross in the x-z plane. This, rather than the shortest distance between tracks, was chosen for convenience in the reanalysis. The distribution depended on the angle of tip of the event out of the plane of the apparatus, and also on the distance of the K_L^o decay point from the target.

4 and 5: The difference between the vertical slopes of the trajectories in front of and behind the magnets, left and right sides respectively. These were corrected for focusing effects of the magnets, and the distributions were treated as dependent on the particle momentum and the intersection of the trajectory with the magnet midplane.

To allow for possible variations with calendar time, the data were broken down into eight sequences of contiguous runs which were then treated independently.

The means and R. M. S. values of the distributions were obtained from $K_L \rightarrow \pi\pi$ candidates. For this purpose clean and essentially unbiased samples were obtained by imposing a mass cut (492-504 MeV/c^2), a range cut (less than the shortest possible range of a muon of the same momentum), and a cut on the horizontal displacement between the front and rear straight line trajectories projected to the magnet midplane (to help eliminate pion decays in flight). These restrictions were removed before the complete data sample was surveyed, using the distribution parameters so obtained.

χ^2 Survey of the Data

Some cuts were applied to all the data:

1. A cut on the horizontal displacement between front and rear tracks projected to the center planes of the magnet, similar in nature to the cut in the last paragraph. The limits were set for convenience at ± 4 to ± 6 standard deviations as determined from the $K\pi\pi$ data. This distribution was shown to be only weakly correlated to the other variables chosen, and the cuts were effective against pion decays in flight and the infrequent cases where the true trajectory had been misidentified because of excessive multiplicity in the front spark chambers.
2. A lower momentum cut on secondary trajectories at 450 MeV/c and an upper limit to the K_L momentum of 3.15 GeV/c, together excluding $< 0.5\%$ of data.
3. Fiducial volume cuts on the K_L decay point as discussed in the previous part of this report.
4. An 8 standard deviation cut at the K_L production target to reduce the number of three-body decays in the data.

$\underline{K_L^o \rightarrow \pi^+\pi^-}$ Events

The $K\pi\pi$ candidates were subdivided into four categories to help in the separation from the remaining $K\mu 3$ events. Since the range telescopes were useful only for momenta above 550 MeV/c, events with a trajectory of momentum less than this were separated from the rest. The data were then further divided according to whether or not the range of any trajectory with momentum above 550 MeV/c was shorter than that of a muon of the same momentum. In no case were both momenta below 550 MeV/c.

Invariant mass plots of these subgroups are illustrated in Fig. 10 for three values of a maximum χ^2 cutoff. The χ^2 distributions are shown in Fig. 11. Note that because of poverty in statistics the low momentum data were analyzed with distribution parameters obtained at a higher mean momentum, and this causes their poor fit to the theoretical χ^2 curve. That the poor distributions for the "muon range" events are caused by $K\mu 3$ contamination is supported by the observation that it is the "target" distributions which cause the failure. Excluding these components from the χ^2 the distributions are acceptable.

The imposition of a limit on permissible χ^2 at 20 excludes less than 1.5% of all the $K\pi\pi$ events. Within this limit and in the mass range $493 < m_{\pi\pi} < 502$ MeV/c^2 there are 820, 869 $K\pi\pi$ events after background subtraction with an uncertainty in the range of $\pm 1\%$.

$\underline{K_L^o \rightarrow \mu^+\mu^-}$ Candidates

Events with mass $m_{\mu\mu}$ between 480 and 510 MeV/c^2 were histogrammed and in most cases those with $m_{\mu\mu}$ greater than 490 MeV/c^2 were examined individually. A simple selection on χ^2 of <30 (or <20) retained a statistically smooth background at a level of ~35 (~25) events per MeV/c^2 at the K mass.

As the next step in the examination of these candidates, their ranges were employed for the first time. The performance of the range telescopes, as noted above, was excellent.[7] Because of multiple scattering in the degrader, a conservative margin of 5 cm was taken at the edges of the sensitive areas of the range counters. If the projected trajectory of a muon at its observed stopping counter fell closer to the edge than this margin, the trajectory was considered unidentifiable. In this case the event was retained for further analysis only if the other projected track stopped at least 10 cm in from the edge of its last range counter. This requirement is similar to the $K\mu 3$ range criterion of the first section of the report. An equivalent condition was required of events where one particle had momentum below 550 MeV/c and was consequently unidentifiable. Events failing this fiducial volume test averaged a rate of 5 per MeV/c^2 ($\chi^2 < 20$) at the K_L mass, and showed no evidence of a $K_{\mu\mu}$ bump.

The majority of the remaining data had a track with no signal in one or both range telescopes where a track of from 2 to 17 counters would be expected. Again these showed no evidence of a K peak, but at a level of $\sim$20 events per MeV/c^2 at the K mass. They were removed from the sample.

The remaining events are illustrated in Fig. 12, where they are divided according to whether or not both eligible ranges exceed a penetration depth of two counters short of the least possible muon range. At this stage in the treatment the analogy between this experiment and the contradictory one is probably at its closest. In anticipation of the normalization of this data it may be noted that the alternative result[3] would require 9^{+6}_{-3} $K\mu\mu$ events in this selection.

Inside the same mass limits as were used to specify $K\pi\pi$ events there are 18 $K\mu\mu$ candidates with ranges > 0 for trajectories inside the margin cuts and

$\chi^2 < 20$. Tightening the range criterion sequentially to (least possible muon range-N counters) N = 6, 4, 2 reduces the number of candidates to 6, 4, and 2 respectively, the last two appearing in Fig. 12(b).

For these 18 events we have considered the probability of an apparent range shortening through multiple scattering, estimating the scattering at the observed end of range by using the experimentally tested numerical integration.[9] All events have at least one trajectory at three or more standard deviations from the edge of the detector. Eight of the 18, however, have both trajectories within five standard deviations of scattering out of the telescopes. Some parameters of the most suspicious candidates are listed in Table V where events 3 and 4 are the entries near 500 MeV/c^2 in Fig. 12(b).

In most of these cases scattering is at least as probable a mechanism for failure as extreme range straggling. Using the empirical information on scattering, range straggling distributions and counter efficiency, the probabilities of the candidates having been $K\mu\mu$ events range downwards from ~0.1%. Further, the trajectory horizontal continuity information from the spectrometers may be introduced at this stage to eliminate event 5 with a discontinuity of more than 5 standard deviations.

The conclusion drawn is that beyond the three standard deviation probability level there are no $K_L \to \mu\mu$ events among these candidates.

The Ratio $R_2 = \Gamma(K_L^o \to \mu^+\mu^-)/\Gamma(K_L^o \to \pi^+\pi^-)$

The simulation program discussed above was used to evaluate the relative acceptances of the 2π and 2μ modes under the conditions of the latter analysis. A simulated $K\mu\mu$ trigger angle distribution is illustrated in Fig. 9(b). The agreement between data and simulation for the $K\pi\pi$ distributions is, of course, good. The relative acceptance ratio for fully efficient apparatus is

$$\frac{A(\pi\pi)}{A(\mu\mu)} = (74.75 \pm 0.56)\%$$

The effect of the inefficiency in the spark chambers, already noted, has been examined in detail and modifies the acceptance ratio to

$$\frac{A(\pi\pi)}{A(\mu\mu)} = (75.35 \pm 0.56)\%$$

The magnet current uncertainty discussed above for the results of the R_1 measurement has a quite small effect here, an uncertainty of $\pm 0.4\%$. The sense is such that an error causing the other branching ratio to be too high as measured would also cause $\Gamma(K\mu\mu)/\Gamma(K\pi\pi)$ to be too high.

The loss of $K\mu\mu$ events caused by multiple scattering out of the range telescopes of the muons inside the projected fiducial volume is 0.28%. A further correction factor for decays in flight of $K\pi\pi$ events increases the observed sample by a factor of 1.382, as determined by the simulation program. Almost all such decays in flight occurring before the final spark chambers caused rejection from the $K\pi\pi$ sample. Consequently, the correction factor is easy to evaluate and can be applied with confidence.

Since the $K\mu\mu$ candidates have all been rejected with probabilities $\lesssim 10^{-3}$, the limit is obtained:

$$R_2 = \frac{\Gamma(K_L^o \to \mu^+\mu^-)}{\Gamma(K_L^o \to \pi^+\pi^-)} \leq \frac{2.3026}{820869} \times \frac{1}{0.9972} \times 0.7535 \times \frac{1}{1.382}$$

$$\leq 1.534 \times 10^{-6} \text{ (90\% C.L.)}$$

Comments and Conclusions

First, concerning the branching fraction of the $K\pi\pi$ channel, Fig. 13 illustrates the published measurements in approximate calendar sequence.[1,2] The most precise of these was actually inferred from a measurement by an amplitude interference technique of $\eta_{+-} = A(K_L^o \to \pi^+\pi^-)/A(K_S^o \to \pi^+\pi^-)$. Ignoring the rather esoteric possibility of secular time dependence of the decay process, there appears to be some latent systematic difficulty in at least one set of experiments. The branching ratio average prior to 1970 was $(0.157 \pm 0.005)\%$, whereas subsequent to 1971 the average is $(0.210 \pm 0.0043)\%$, eight standard deviations apart. The result here is hardly compatible with either the old measurements (2.7 standard deviations) or the new (3.1 standard deviations).

The reanalysis of the dimuon search data has also failed to resolve its conflict. Errors have been uncovered in the original analysis,[3] notably an erroneous subtraction of the momentum dependent $K\mu 3$ background to the $K\pi\pi$ events, and in the simulation program. One consequence has been that the number of $K\pi\pi$ events used for normalization has decreased. Also the correction to the K_L^o spectrum (which now resembles the $K^\pm$ production spectra acceptably) and the corrected simulation program have combined to lower the calculated sensitivity of the experiment. The result originally quoted was too optimistic by about 24%. This is totally inadequate to close the gap between the two results. The highest joint probability of agreement is 3.5×10^{-4} for a hypothetical branching ratio of $R_2 = 2.9 \times 10^{-6}$.

With respect to the question of the unitarity limit[5,12] the situation is clouded principally by the uncertainty of the $K\pi\pi$ branching fraction R_1. For this reason three values are quoted as possible results from this experiment:

If $R_1 = 1.57 \times 10^{-3}$, $\Gamma(K_L^o \to \mu^+\mu^-)/\Gamma(K_L^o \to \text{all}) < 2.41 \times 10^{-9}$

If $R_1 = 1.82 \times 10^{-3}$, $\Gamma(K_L^o \to \mu^+\mu^-)/\Gamma(K_L^o \to \text{all}) < 2.8 \times 10^{-9}$

If $R_1 = 2.10 \times 10^{-3}$, $\Gamma(K_L^o \to \mu^+\mu^-)/\Gamma(K_L^o \to \text{all}) < 3.22 \times 10^{-9}$,

the limits being at 90% C.L.

Since the unitarity calculation, based on $K_L^o \rightarrow \gamma\gamma$ and $\pi^+\pi^-\gamma$ rate measurements, imposes a lower limit on the $K_L^o \rightarrow \mu^+\mu^-$ branching ratio of 5.5×10^{-9} (assuming $|\eta_{00}| = 2.0 \times 10^{-3}$ to be conservative), the agreement of the above numbers with theory is at probability levels of 0.52%, 1.1%, and 2.0% respectively.

Acknowledgments

The original data taking and analysis were performed by the group referred to frequently in this report: A.R. Clark, T. Elioff, R.C. Field, H.J. Frisch, R.P. Johnson, L.T. Kerth and W.A. Wenzel. I wish to thank the group for their encouragement in this revision of the old data. The burden of computing was lightened considerably by J.P. Wilson at LBL where this work was initiated.

REFERENCES

1. J.H. Christenson, J.W. Cronin, V.L. Fitch, and R. Turlay, Phys. Rev. Letters 13, 138 (1964). See the Particle Data Group listing, Phys. Letters 50B, No. 1 (1974) for subsequent work.

2. R. Messner, R. Morse, U. Nauenberg, D. Hitlin, J. Liu, R. Piccioni, M. Schwartz, S. Wojcicki, and D. Dorfan, Phys. Rev. Letters 30, 876 (1973);

   C. Geweniger, S. Gjesdal, G. Presser, P. Steffen, J. Steinberger, F. Vannucci, H. Wahl, F. Eisele, H. Filthuth, K. Kleinknecht, V. Lüth, and G. Zech, Phys. Letters 48B, 487 (1974);

   D.R. Nygren, review given at the Berkeley Conference 1973, A.I.P. Conference Proceedings No. 14, P.P.F. Subseries No. 6, p. 20, American Institute of Physics, New York, 1973.

3. A.R. Clark, T. Elioff, R.C. Field, H.J. Frisch, R.P. Johnson, L.T. Kerth, and W.A. Wenzel, Phys. Rev. Letters 26, 1667 (1971).

4. W.C. Carithers, T. Modis, D.R. Nygren, T.P. Pun, E.L. Schwartz, H. Sticker, J. Steinberger, P. Weilhammer, and J.H. Christenson, Phys. Rev. Letters 30, 1336 (1973);

   W.C. Carithers, D.R. Nygren, H.A. Gordon, M.L. Ioffredo, K.-W. Lai, and P. Weilhammer, Phys. Rev. Letters 31, 1025 (1973).

5. N. Christ and T.D. Lee, Phys. Rev. D4, 209 (1971).

6. A.R. Clark et al., Ref. 3;

   R.P. Johnson, U.C. Berkeley Ph. D. Thesis, UCRL-19709 (April 1970);

   H.J. Frisch, U.C. Berkeley Ph. D. Thesis, UCRL-20264 (March 1971).

7. A.R. Clark, R.C. Field, H.J. Frisch, W.R. Holley, R. P. Johnson, L.T. Kerth, R.C. Sah, and W.A. Wenzel, Phys. Letters 41B, 229 (1972); R.C. Field, LBL-791 (April 1972).

8. D.E. Coyle, R.C. Field, J.T. Gunn, and J.T. Tanabe, Nucl. Instr. Meth. 95, 557 (1971).

9. G. Shen and R.C. Field, Lawrence Berkeley Laboratory Internal Report BeV-3000, Jan. 1973.

10. E.S. Ginsberg, Phys. Rev. 171, 1675 (1968); Errata Phys. Rev. 174, 2169 (1968); Phys. Rev. 187, 2280 (1969).

11. Particle Data Group, Phys. Letters 50B, No. 1 (1974).

12. H. Stern and M. K. Gaillard, Annals of Physics 76, 580 (1973).
G. Donaldson, D. Hitlin, R. Kennelly, J. Kirkby, J. Liu, A. Rothenburg, and S. Wojcicki, "Observation of the Decay $K_L^o \to \pi^+\pi^-\gamma$," Stanford Linear Accelerator Center preprint no. SLAC-PUB-1447 and Ref. 11.

FIGURE CAPTIONS

1. Apparatus, plan view. H is an array of horizontal scintillators, F and R are hodoscopes of vertical scintillators used to define the trigger angle, and T is a counter used for tight timing.
2. K_L^o momentum spectrum.
3. Cerenkov counter and range telescope, elevation view.
4. Muon range distribution showing nominal cutoff. Abscissa is: observed range minus shortest expected muon range.
5. (a) Mass distribution for $K\pi\pi$ class events.

   (b) Mass distribution for $K\pi\pi\mu$ class events.
6. Longitudinal decay distribution of $K\pi\pi$ events.
7. Pion spectrum for $K\pi\pi$ events.
8. Hodoscope trigger angle distribution for $K\pi\pi$ events. Negative angles signify convergence with the beam axis.
9. (a) Hodoscope trigger angle distributions for pions from $K\mu 3$.

   (b) Hodoscope trigger angle distributions for pions from Ke3. The smooth curve represents the simulated $K\mu\mu$ distribution and illustrates the overlap between the Ke3 and $K\mu\mu$ cases.
10. Invariant mass distributions of $K\pi\pi$ candidates for three values of the χ^2 cutoff.

    (a) Both momenta > 550 MeV/c; both ranges $<\mu$ range.

    (b) Both momenta > 550 MeV/c; either range $\geq \mu$ range.

    (c) Either momentum < 550 MeV/c; both ranges $<\mu$ range.

    (d) Either momentum < 550 MeV/c; either range $\geq \mu$ range.
11. χ^2 distributions for the $K\pi\pi$ candidates. Ideal curves for χ^2 of five variables and three variables are shown. The production target variables are dropped from the five-variable to form the three-variable χ^2. The divisions (a)-(d) are as in Fig. 10.

12. Mass distributions of $K\mu\mu$ candidates.

(a) For trajectories with momentum > 550 MeV/c inside the fiducial volume, range is greater than zero but more than two counters short of the least possible muon range.

(b) As (a) except that either range is longer than the upper limit in (a).

13. Experimental results on the $K\pi\pi$ branching ratio R_1, in approximate calendar sequence of data acquisition. See Ref. 1 and 2. Open circle denotes this experiment. Note the suppressed zero of the ordinate.

TABLE I

List of Cuts Common to All Data

1. Trajectories projected from front and rear met at the magnet centre plane within ±2.0 cm horizontally, ±1.0 cm vertically.

2. Front trajectories passed through the vacuum box window.

3. The vertex lay within ±17.8 cm vertically and horizontally of the beam axis.

4. In the range 762 cm to 813 cm from the target (near the entrance to the decay volume), the vertex lay within ±10.2 cm vertically and horizontally of the beam axis.

5. Secondary momenta lay between 0.55 GeV/c and 1.8 GeV/c.

TABLE II

Category	$K\pi\pi$ Tests (Invariant Mass, Target)	μ Test (range)	e Test (Cerenkov)
1 : $K\pi\pi$	Yes	No	No
2 : $K\pi\pi\mu$	Yes	Yes	No
3 : $K\pi\pi C$	Yes	No	Yes
4 : $K\mu 3$	No	Yes	No
5 : $K\mu 3$ C1	No	Yes	Yes, π side
6 : $K\mu 3$ C2	No	Yes	Yes, μ side
7 : Ke3	No	No	Yes
8 : XXX	No	No	No

TABLE III

Breakdown of Identification Categories

Identification	Label	7.5 cm cut	12.5 cm cut
$K_L \to \pi\pi$	$K\pi\pi$	24517 ± 249	19575 ± 188
	$K\pi\pi\mu$	4446 ± 235	3314 ± 200
	$K\pi\pi C$	280 ± 20	202 ± 25
	Total	29243 ± 343	23091 ± 282
$K_L\mu3$	$K\pi\pi$	385 ± 193	250 ± 125
	$K\pi\pi\mu$	4857 ± 235	4062 ± 200
	$K\mu3$	78260 ± 280	58803 ± 243
	$K\mu3$ C1	472 ± 400	400 ± 400
	$K\mu3$ C2	132 ± 25	94 ± 20
	Total	84106 ± 577	63609 ± 565
K_Le3	$K\pi\pi C$	733 ± 34	539 ± 31
	$K\mu3$ C1	4245 ± 405	3390 ± 400
	$K\mu3$ C2	287 ± 30	239 ± 25
	Ke3	41126 ± 203	31920 ± 179
	Total	46391 ± 455	36088 ± 444

TABLE IV

Data Samples and Corrections

	7.5 cm cut	12.5 cm cut
$K\pi\pi$:		
Raw events	29243 ± 343	23091 ± 282
Correction for Cerenkov losses	+994 ± 116	+805 ± 92
Correction for decay in flight	× (1.38 ± 0.025)	× (1.38 ± 0.025)
Total	41728 ± 906	32976 ± 724
$K\mu 3$:		
Raw events	84106 ± 577	63609 ± 565
Correction for Cerenkov losses	+3070 ± 349	+2283 ± 252
Subtraction of background from $K\pi\pi$ with π decay in flight	-1834 ± 183	-1449 ± 145
Correction for μ multiple scattering losses	× 1.0152	× 1.003
Correction for π decay in flight	× (1.14 ± 0.014)	× (1.14 ± 0.014)
Total	98768 ± 1458	73685 ± 1160
Ke3:		
Raw events	46391 ± 455	36088 ± 444
Correction for Cerenkov losses of pions	+501 ± 45	+390 ± 35
Correction for bremsstrahlung	× (1.027 ± 0.003)	× (1.027 ± 0.003)
Correction for π decay in flight	× (1.14 ± 0.014)	× (1.14 ± 0.014)
Corrected Total	54900 ± 951	42708 ± 804

TABLE V

Parameters of Best $K_L^o \rightarrow \mu^+ \mu^-$ Candidates

Mass	χ^2	Right Range D	Right Range P	Left Range D	Left Range P
1. 494.0	7.01	3	7×10^{-5}	12	0.17
2. 495.2	10.82	3	1×10^{-3}	11	0.095
3. 499.8	9.00	1	0.2*	1	7×10^{-5}
4. 499.8	6.55	8	0.35	1	1.4×10^{-3}
5. 500.9	17.94	5	0.55	8	1.4×10^{-3}
6. 501.2	1.78	12	0.19	8	9.5×10^{-4}

D--Number of counters by which range falls short of the least possible muon range (defined at the 3 standard deviation point on the straggling distribution). One counter $\simeq$2.5 standard deviations.

P--Probability of muon escaping from range telescope at the observed end-of-range by multiple scattering.

* In the track counters 2, 9, 10, 11 were present. The probability of scattering out at the beginning of the telescope is 0.038.

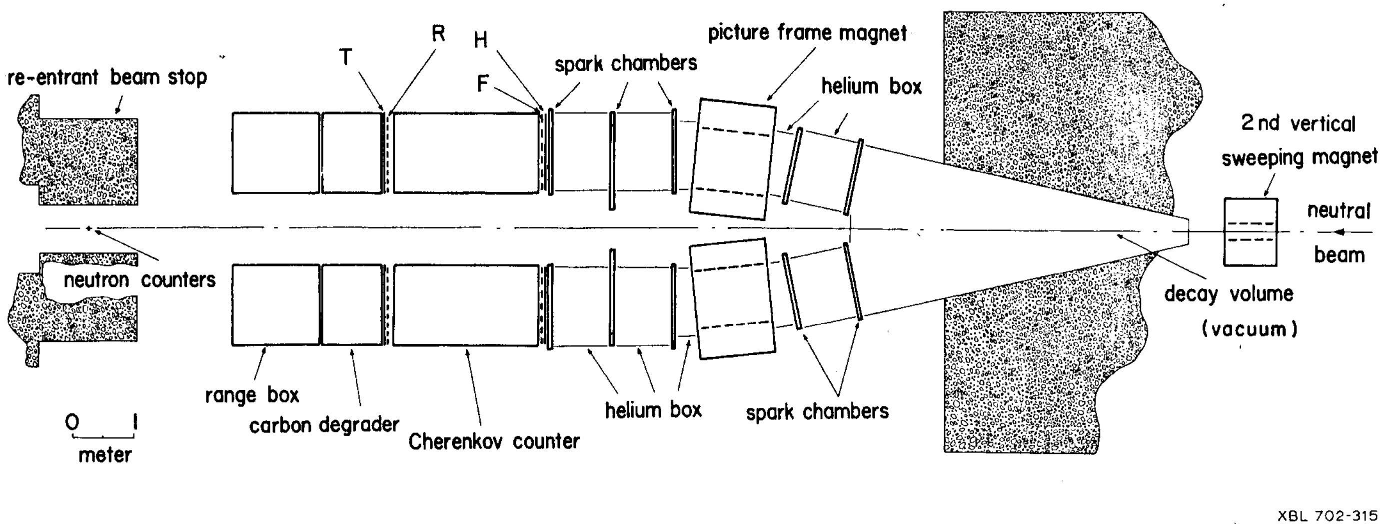
re-entrant beam stop
T
R
H
F
spark chambers
picture frame magnet
helium box
2nd vertical
sweeping magnet
neutral
beam
neutron counters
decay volume
(vacuum)
range box
carbon degrader
Cherenkov counter
helium box
spark chambers
0
1
meter
XBL 702-315

Fig. 1

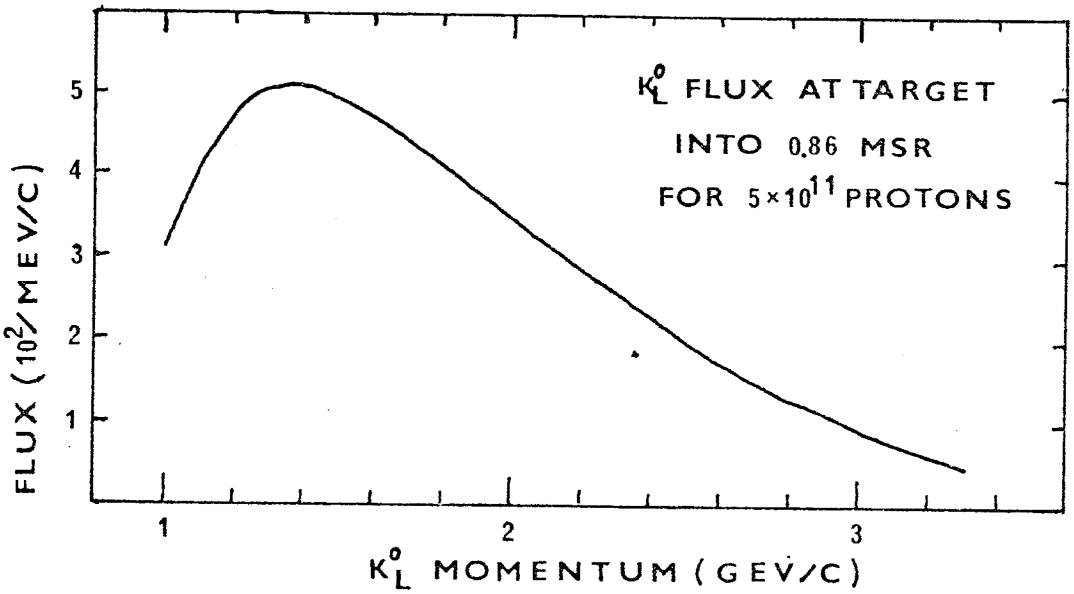

XBL 735-655

Fig. 2

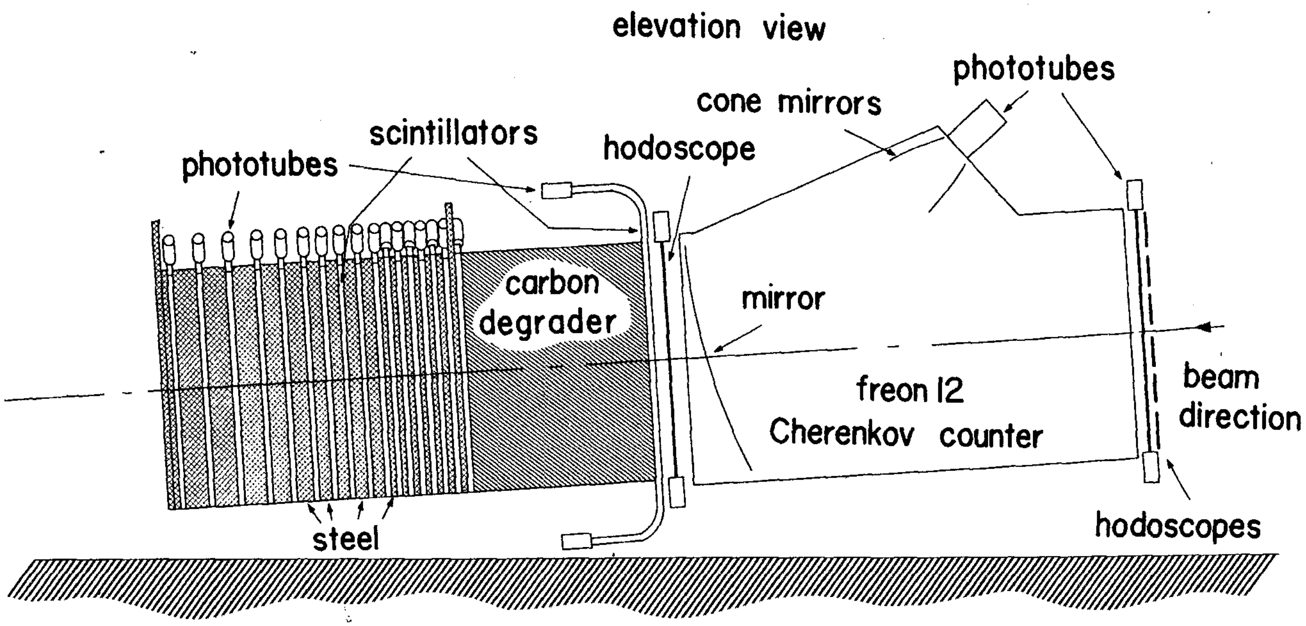

XBL 702-316

Fig. 3

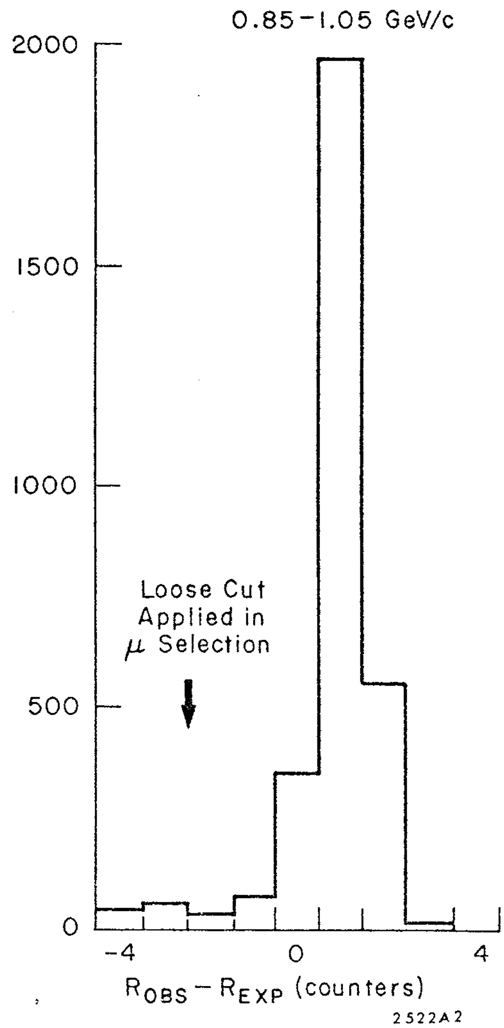
0.85-1.05 GeV/c
2000
1500
1000
500
0
Loose Cut
Applied in
μ Selection
-4
0
4
R_OBS - R_EXP (counters)
2522A2

Fig. 4

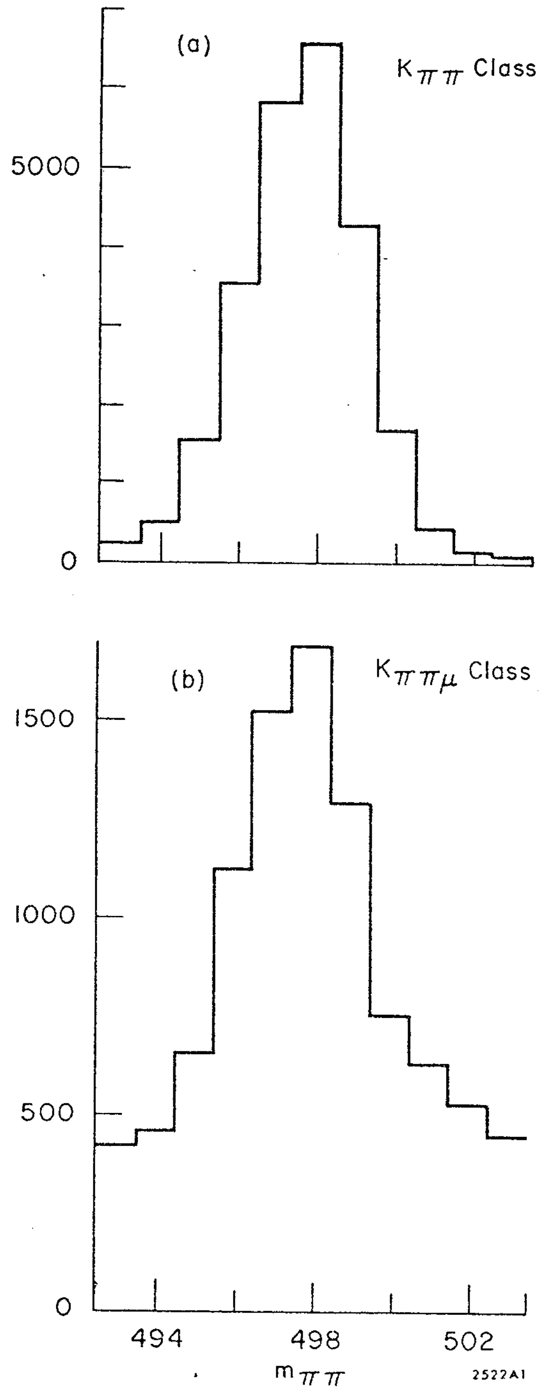

(a)
$K_{\pi\pi}$ Class
5000
0
(b)
$K_{\pi\pi\mu}$ Class
1500
1000
500
0
494
498
502
$m_{\pi\pi}$
2522A1

Fig. 5

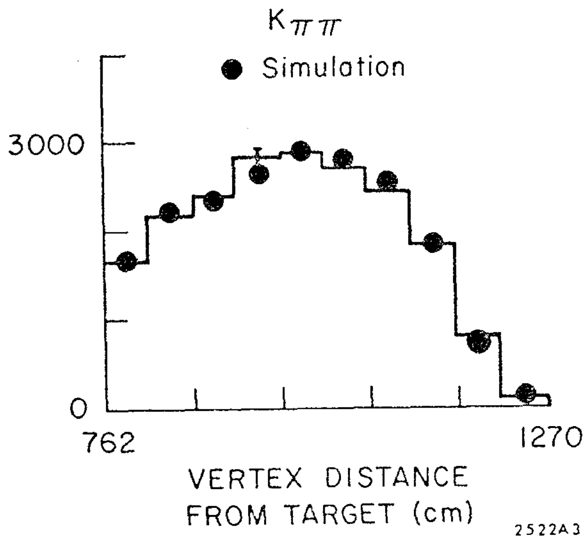

$K_{\pi\pi}$
Simulation
3000
0
762
1270
VERTEX DISTANCE
FROM TARGET (cm)
2522A3

Fig. 6

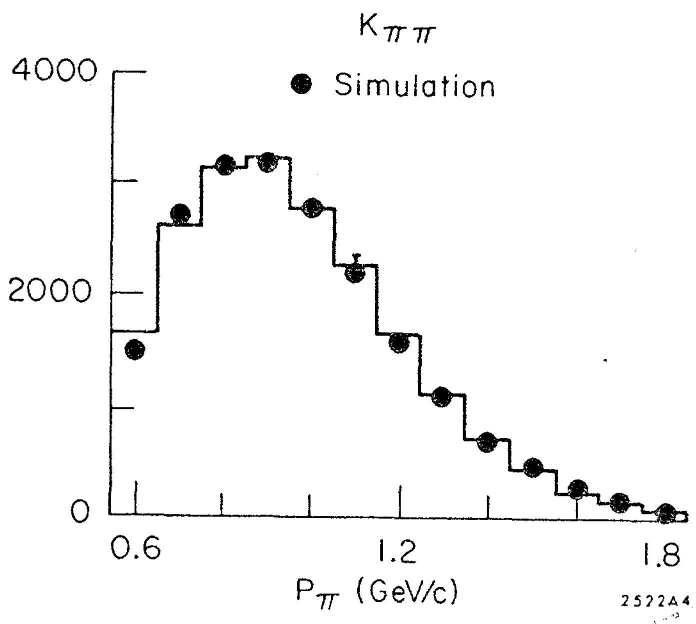

Fig. 7

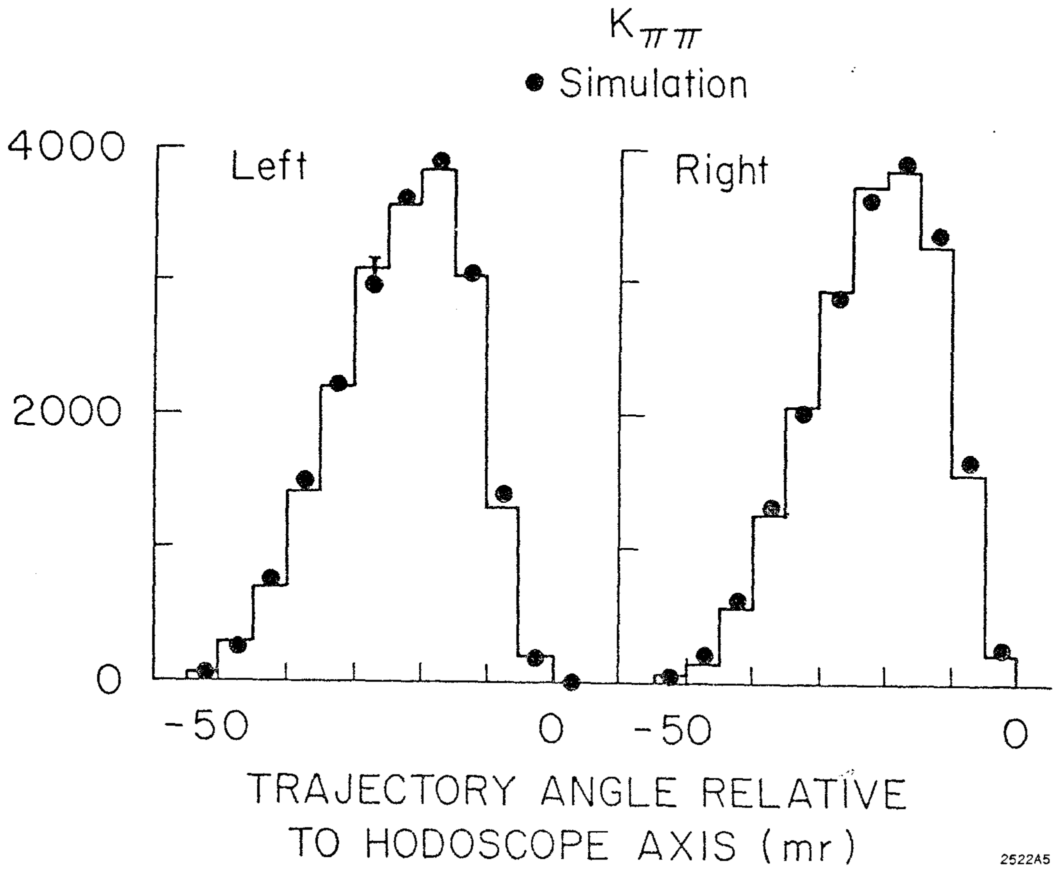

$K_{\pi\pi}$
● Simulation
4000
2000
0
Left
Right
-50
0
-50
0
TRAJECTORY ANGLE RELATIVE TO HODOSCOPE AXIS (mr)
2522A5

Fig. 8

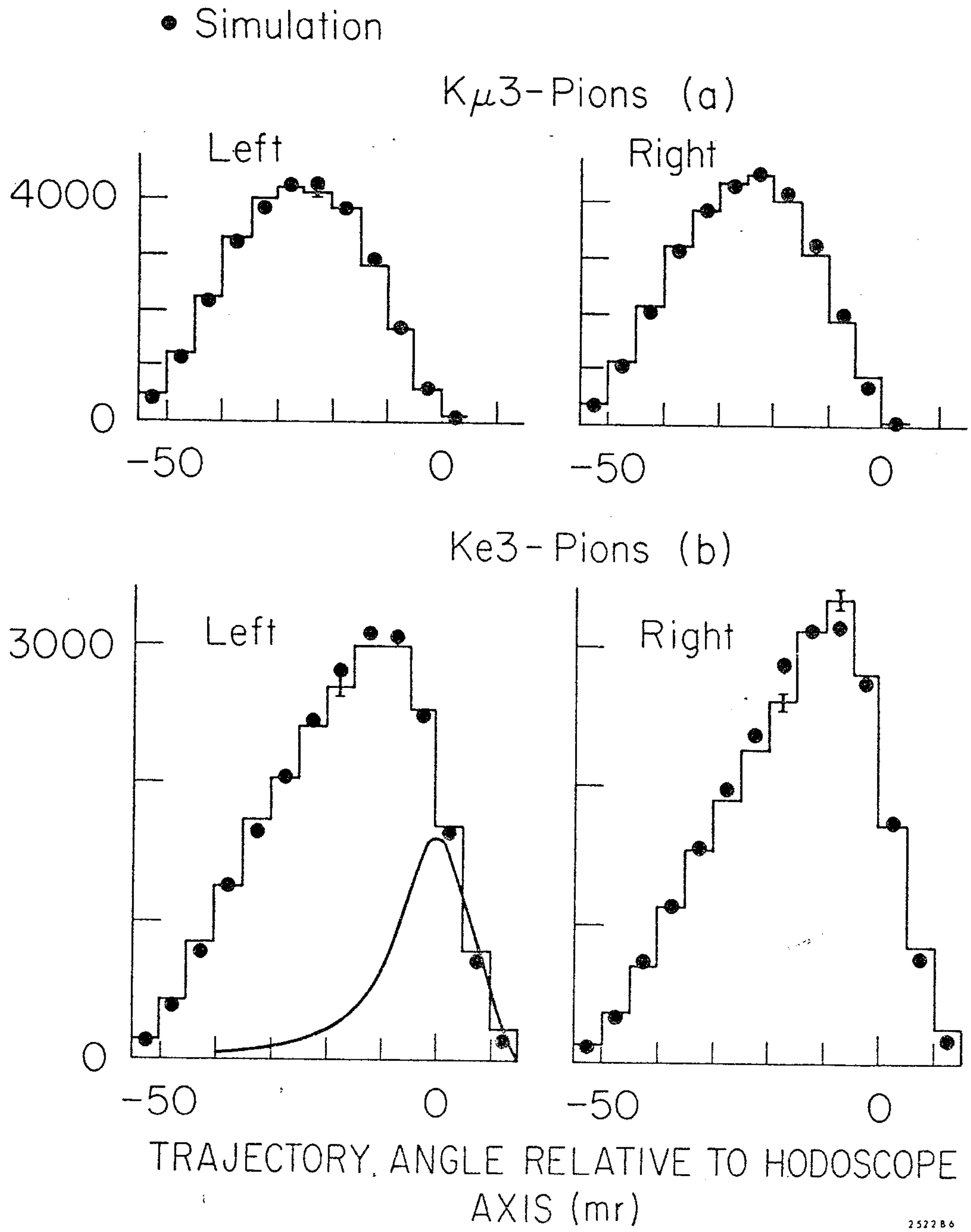

• Simulation
Kμ3-Pions (a)
Left
Right
4000
0
−50
0
−50
0
Ke3-Pions (b)
Left
Right
3000
0
−50
0
−50
0
TRAJECTORY ANGLE RELATIVE TO HODOSCOPE AXIS (mr)
252286

Fig. 9

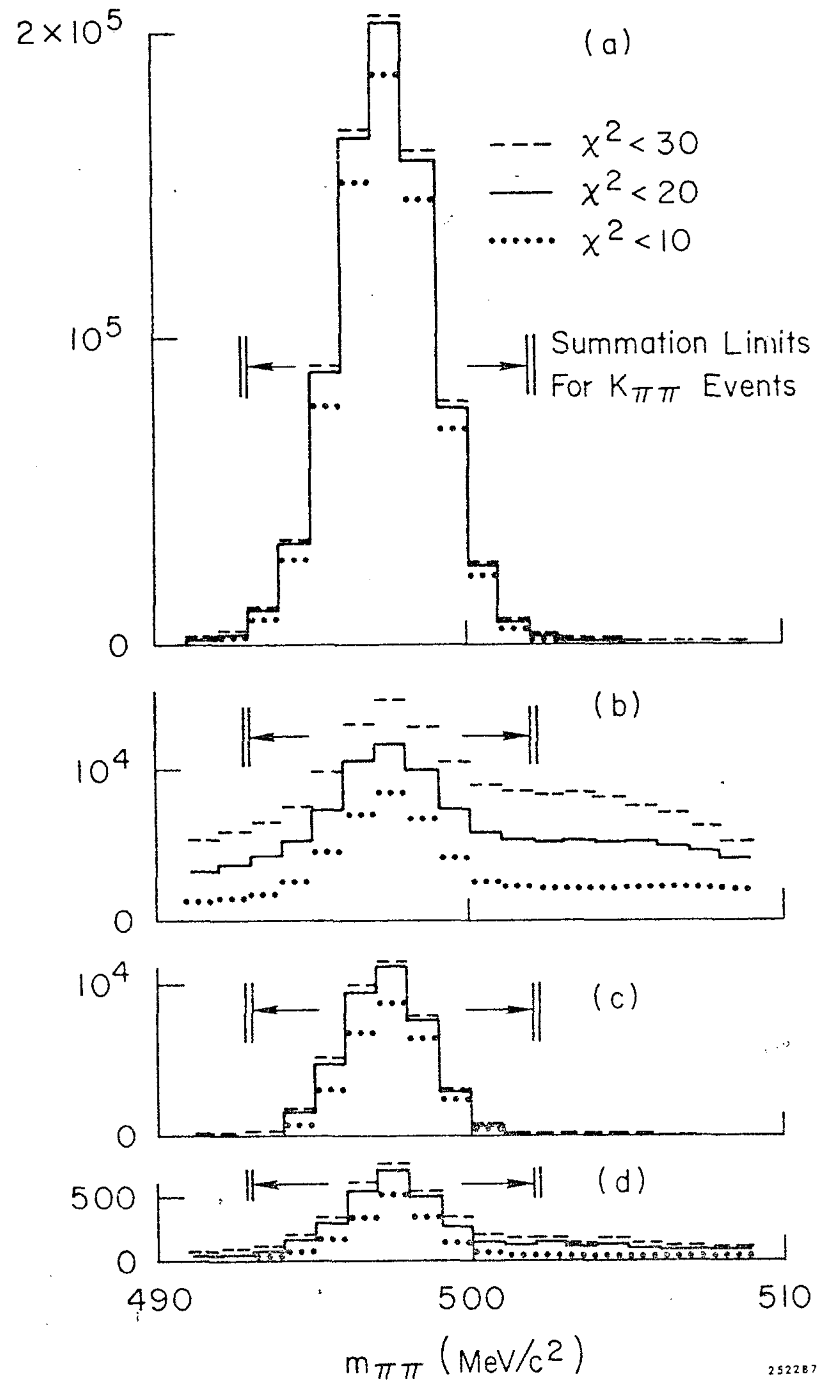

2×10^5
(a)
χ^2 < 30
χ^2 < 20
χ^2 < 10
10^5
Summation Limits
For Kππ Events
0
(b)
10^4
0
10^4
(c)
0
(d)
500
0
490
500
510
mππ (MeV/c^2)
252287

Fig. 10

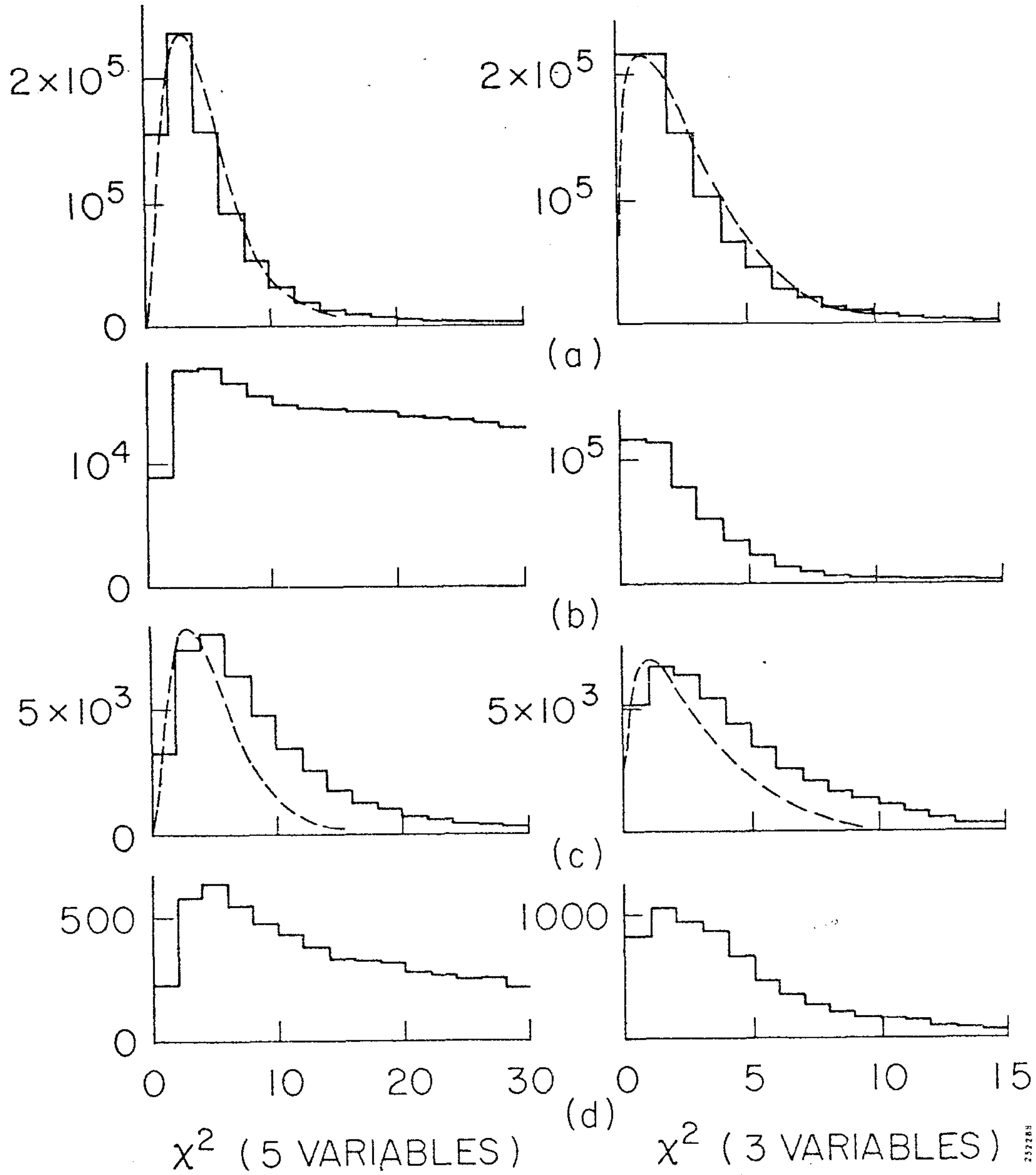

2×10^5
10^5
0
(a)
10^4
10^5
0
(b)
5×10^3
5×10^3
0
(c)
500
1000
0
0
10
20
30
0
5
10
15
(d)
χ^2 (5 VARIABLES)
χ^2 (3 VARIABLES)

Fig. 11

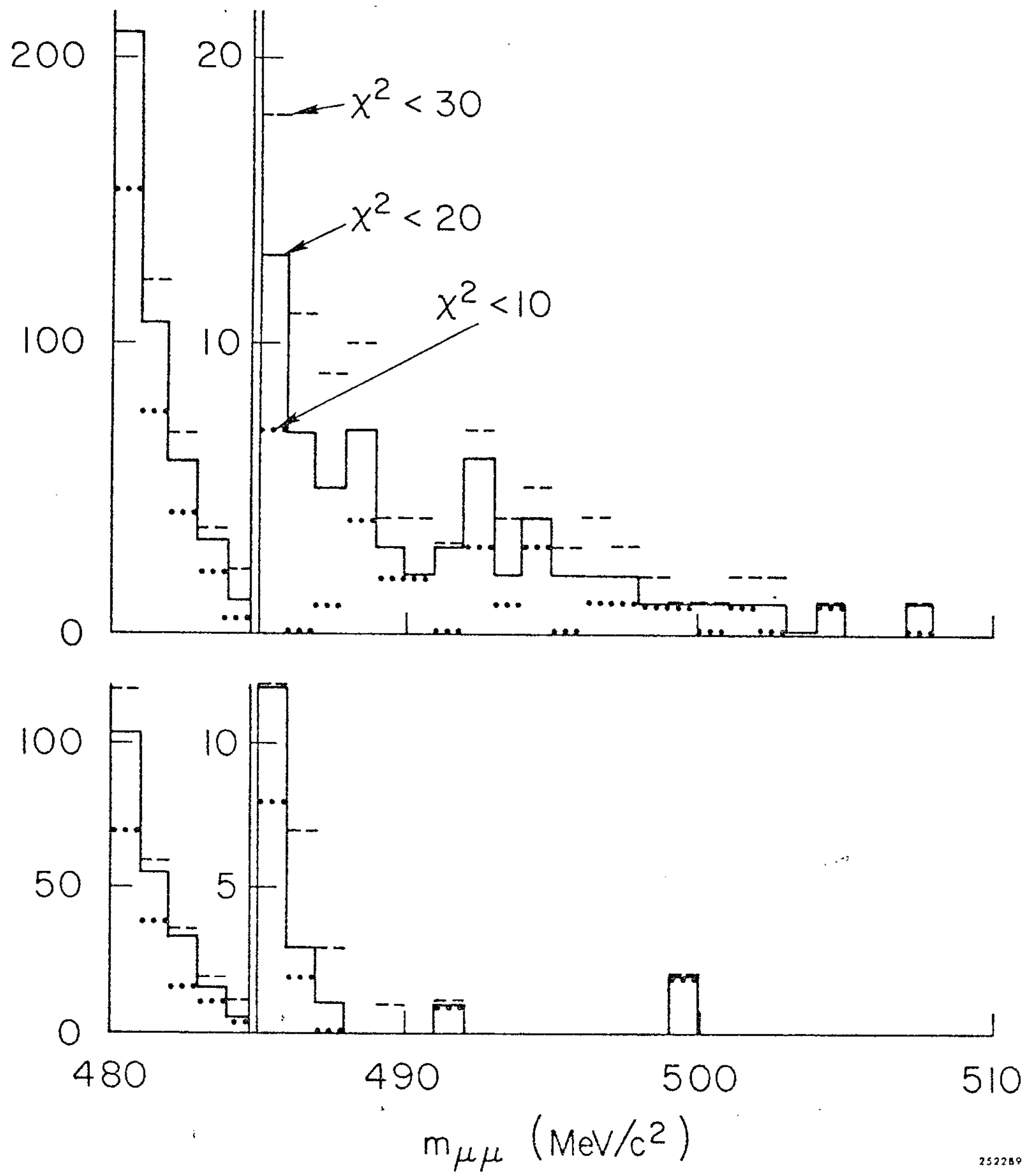

200
100
0
20
10
$\chi^2 < 30$
$\chi^2 < 20$
$\chi^2 < 10$
100
50
0
10
5
480
490
500
510
$m_{\mu\mu}$ (MeV/c^2)
252289

Fig. 12

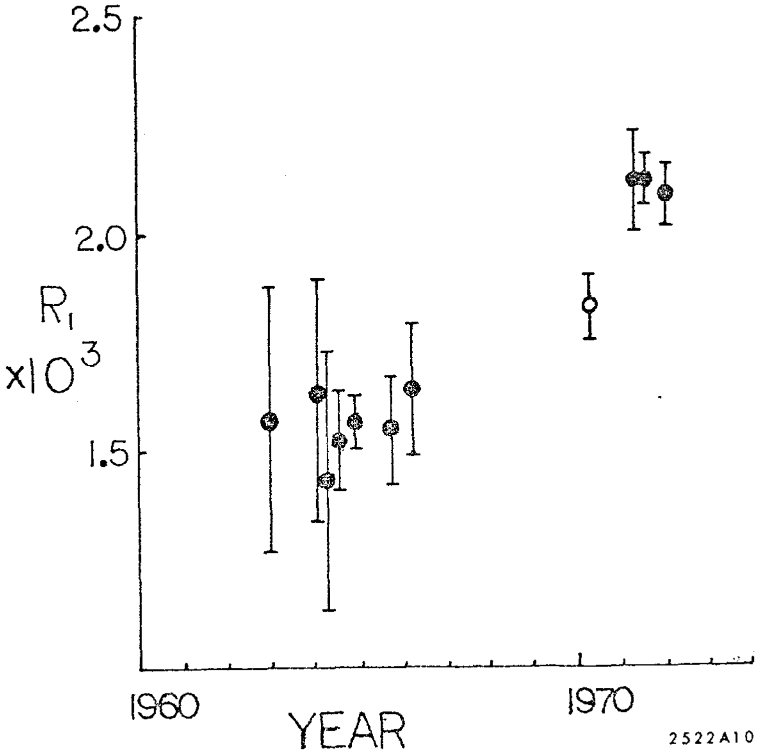

Fig. 13